EFFECT OF FRICTION ON A RECEDING CONTACT BETWEEN CYLINDRICAL INDENTER, LAYER AND SUBSTRATE

Rončević B., D.Sc.
Faculty of Engineering – University of Rijeka, Croatia
E-mail: branimir.roncevic@riteh.hr

Abstract: *This paper presents the results of a finite element analysis of a receding frictional contact between a cylindrical indenter, layer and substrate. The elasticity of all three bodies is taken into account, and the bodies are considered as isotropic. The problem is analysed within the frame of linear theory of elasticity and under the assumption of plane strain conditions. It is a well known fact that the presence of friction modifies the resulting contact pressure distributions, and the results obtained for the case of elasticity of all three bodies presents a novelty in this field of study. Furthermore, the results are analysed for several different geometries, which gives an insight into the influence of the ratio between the indenter radius and layer thickness.*

KEYWORDS: *RECEDING CONTACT PROBLEM, FRICTIONAL CONTACT, UNBONDED LAYER, CYLINDRICAL INDENTER*

1. Introduction

In most contact problems the area of the contact surface increases as the intensity of the applied load and the ensuing deformation also increase. However, a separate class of conforming contact problems deviates from this behaviour; in these cases the contact area shrinks with the application of load. Such contacts are referred to as receding contacts. In a more succinct definition given by K. L. Johnson, a receding contact is one where the loaded contact area is completely contained within the unloaded contact area [1]. Receding contact typically occurs in structural problems involving unbonded layers pressed against a substrate. This type of structural problem is mainly encountered in foundations, pavements and railways, but it has also been studied in connection to tilting pad bearings and resistance spot welding problems, thus making it a model problem relevant in quite a wide range of technological fields.

This problem was studied extensively in scientific literature over the past few decades. The discovery of the phenomenon can be attributed to Filon [2], and some of the more important analytical studies that set the theoretical basis for further research can be found in [3-5]. An interesting experimental study from that period carried out by Durelli, Parks and Nørgård is found in [6]. Among the newer studies, results found in [7-12] can be singled out. The common feature of all results published over the span of an entire century is that the problem was always considered with certain simplifications that made analytical solutions possible or numerical analyses somewhat less demanding; in some cases the indenter was replaced by a concentrated force or a uniformly distributed pressure of constant width, while in some cases either the indenter or both the indenter and the support were assumed as rigid. The most recent study by Rončević et al. in [13] was carried out free of these restrictions for the case without friction, and the obtained results showed marked differences from the idealized solutions. This is primarily because the elasticity of the indenter leads to the case of load-dependent contact widths, whose extent progresses faster than in the case of rigid indenter, and consequently lower values of maximal contact pressures are obtained. As a continuation of the research presented in [13], the case of a frictional receding contact remains to be systematically scrutinized.

This paper considers the case of an elastic cylindrical indenter pressing an unbonded elastic layer resting on an elastic support. The problem is modelled under the assumption of linear elasticity and plane strain, with friction also taken into account. This implies that in addition to compressive tractions both contacting surfaces (i.e. indenter-layer, layer-support) transmit tractions in the tangential direction as well. All bodies in contact (indenter, layer and substrate) are assumed to be isotropic, with the elasticity of the indenter leading to continuous change of the contact width as load is increased. The analysis is carried out in a preliminary fashion, with emphasis on the qualitative aspect of the problem. In Chapter 2 a brief description of the problem and numerical model is outlined. Analysis results are presented and discussed in Chapter 3. Chapter 4 gives concluding remarks, complemented by an outlook to future research.

2. Numerical model

2.1. Description of the problem

The problem investigated in this research is shown in Fig. 1. An indenter with a cylindrical profile of radius R is loaded by a uniformly distributed stress $\sigma = 10^8$ N/mm, thus pressing against the layer that rests unbonded on top of flat support. After being subjected to the pressure exerted by the indenter over a contact area of the width $2a$, the layer separates from the substrate, maintaining contact with it only over the contact area of the width $2b$.

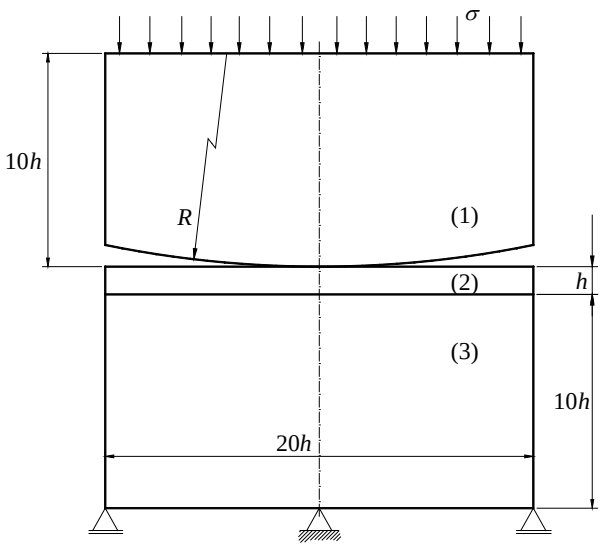

Fig. 1. *Geometry of the problem: (1) indenter, (2) layer, (3) substrate (support)*

The primary unknowns are the half-widths of the two contact areas, i.e. a at the indenter-layer interface and b at the layer-substrate interface, contact pressure distributions (normal p_n and tangential p_t) on both contact surfaces, and finally the extent of stick and slip zones, which is also a matter of interest.

2.2. Features of the finite element model

Material properties of all three bodies are assumed to be the same, namely: $E = 200$ GPa, $\nu = 0.3$. Four different geometries are analysed by varying the indenter radius R, with the remaining measures and proportions kept as shown in Fig. 1; these geometries correspond to ratios $R/h = 50$, 100, 200 and 500.

The coefficient of friction on both contacting surfaces is taken as $\mu = 0.2$, and the transition from the state of stick to the state of slip is assumed to take place in accordance with Coulomb's friction model. This means that the static friction (stick) at any given point on the contact surface is overcome (slip) when the tangential traction p_t reaches the value μp_n, with p_n being the normal contact traction.

For the purpose of FEM analysis, the material of all three contacting bodies is defined as isotropic and linearly elastic and the model is solved by using the nonlinear static analysis in the Femap software package. The model is meshed with plane strain finite elements, which is an especially suitable approximation for the modelling of the layer. A detail of the mesh in the vicinity of the initial point of contact is shown in Fig. 2, showing the uniform structuring of the mesh in the region where accuracy of the result is of utmost importance.

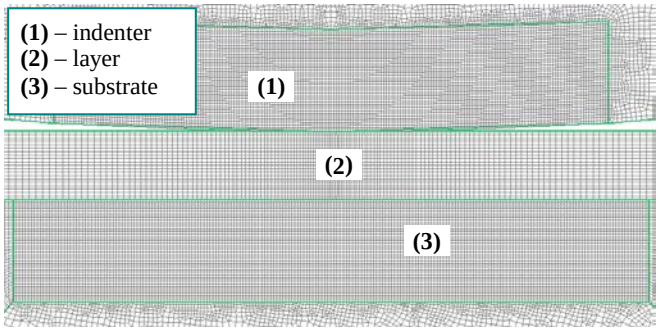

Fig. 2. *Mesh detail around the initial point of contact*

The transmission of forces between the contacting bodies is modelled by using *slide line* elements, which offer several important advantages over the limiting capabilities of the now outdated gap elements. Slide line elements easily deal with non-conforming meshing (node-on-element) and also allow large displacements of the contacting surfaces in the tangential direction (i.e. along the slide line). Every slide line element can contain an arbitrary number of nodes that are lying on the lines or curves of both bodies where the contact forces are transmitted or are expected to take place with the application of load. The nodes of one body are designated as the *master nodes* and the nodes of the other as the *slave nodes*, the choice between the two usually being arbitrary. The Femap algorithm uses the penalty method for imposing the displacement compatibility conditions and the calculation of the contact forces [14,15].

3. *Analysis results*

In order to assess how the presence of friction influences the resulting contact pressure distributions, it is useful to partly reproduce the already obtained results for the frictionless case, given in [13]. For geometry $R/h = 50$ contact pressure distributions are shown in Fig. 3 in dimensionless form. Hereafter, it will be understood that index 1 designates the indenter-layer interface, and index 2 designates the layer-substrate interface.

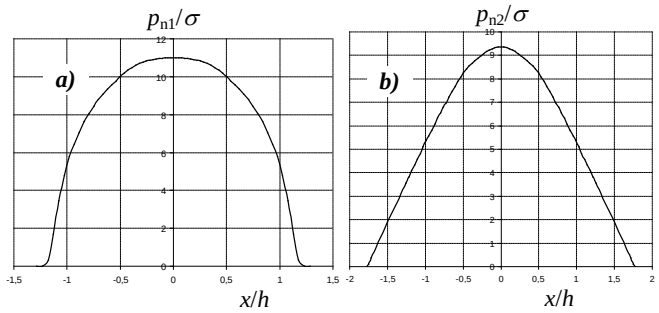

Fig. 3. *Contact pressure distributions for the frictionless case and geometry $R/h = 50$: a) at the indenter-layer interface $a/h \approx 1.29$ and $p_{n1,max}/\sigma \approx 11$; b) at the layer-substrate interface $b/h \approx 1.78$ and $p_{n2,max}/\sigma \approx 9.35$*

For the remaining geometries in case with no friction the results are qualitatively similar to those given in Fig. 3, and the values of contact half-widths and maximal contact pressures are given in Table 1. It should be kept in mind that the results in Table 1 exist only for the normal contact pressures, due to the absence of friction.

The results obtained for the case of frictional contact can then be compared to the results from Fig. 1 and Table 1.

Table 1. *Results for the frictionless contact (approximate values)*

R/h	a/h	$p_{n1,max}/\sigma$	b/h	$p_{n2,max}/\sigma$
100	1.70	7.768	2.13	7.358
200	2.40	5.526	2.70	5.481
500	3.71	3.626	3.96	3.574

The contact pressure distributions obtained for the frictional contact are shown in Figures 4-7. The dashed line in these figures represents the local static friction force, i.e. the threshold for the occurrence of slip state at any observed point of the contact area when the local tangential force reaches this value.

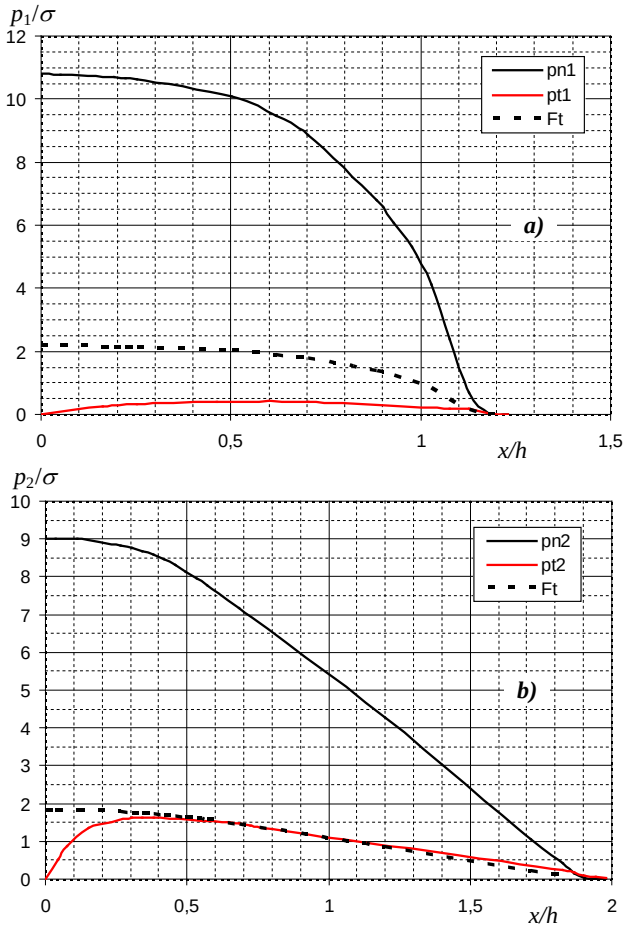

Fig. 4. *Contact pressure distributions for $R/h = 50$;*
a) at the indenter-layer interface $a/h \approx 1.24$, $p_{n1,max}/\sigma \approx 10.8$;
b) at the layer-substrate interface $b/h \approx 1,99$, $p_{n2,max}/\sigma \approx 9$

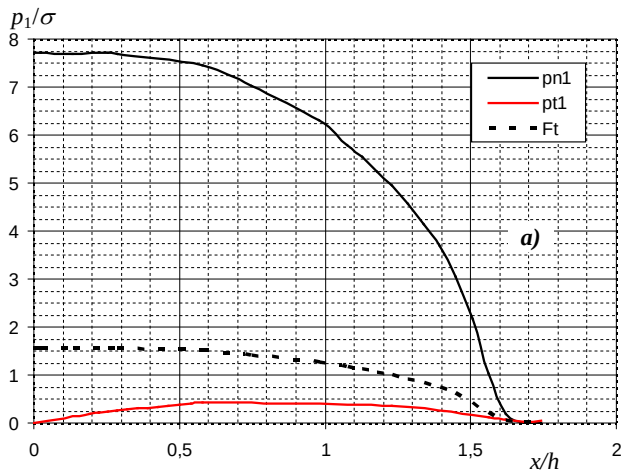

Fig. 5. *Contact pressure distributions for $R/h = 100$;*
a) at the indenter-layer interface $a/h \approx 1.74$, $p_{n1,max}/\sigma \approx 7.71$;

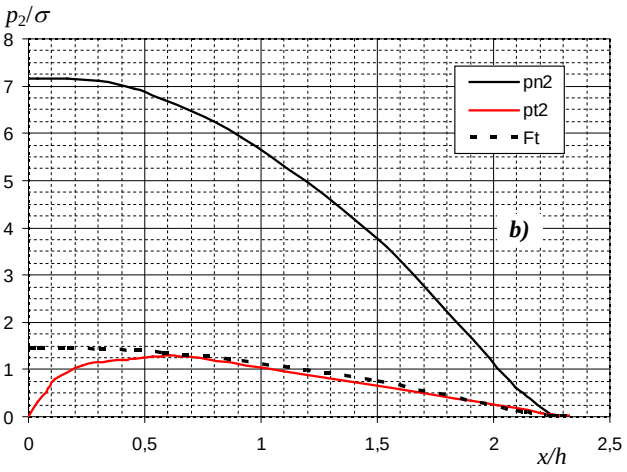

Fig. 5. *(continued) Contact pressure distributions for R/h = 100;*
b) at the layer-substrate interface b/h ≈ 2.32, $p_{n2,max}/\sigma \approx 7.16$

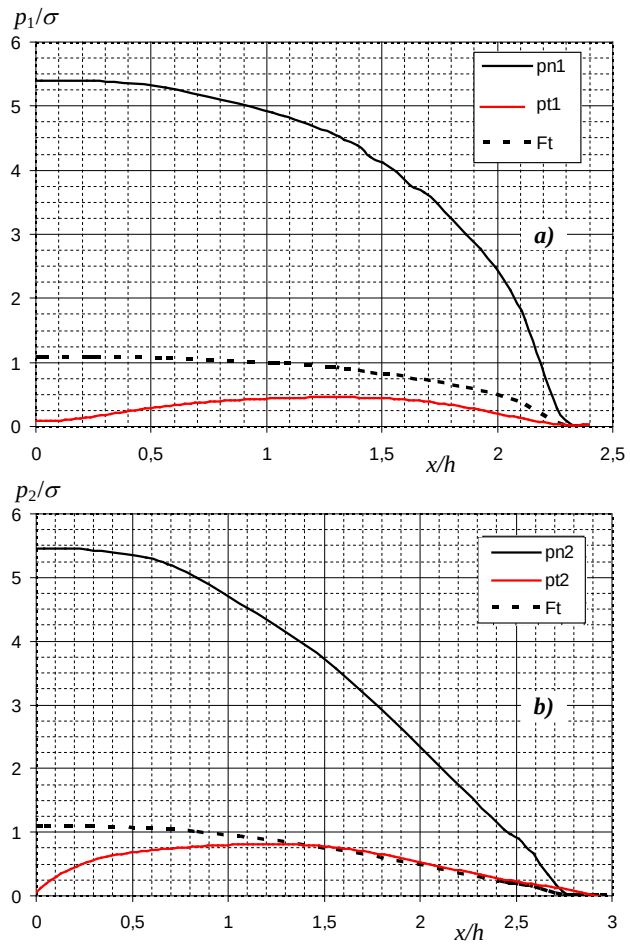

Fig. 6. *Contact pressure distributions for R/h = 200;*
a) at the indenter-layer interface a/h ≈ 2.41, $p_{n1,max}/\sigma \approx 5.4$;
b) at the layer-substrate interface b/h ≈ 2.97, $p_{n2,max}/\sigma \approx 5.45$

The distribution of tangential contact tractions p_t (the red line) in Figs 4.b and 6.b goes slightly above the line of the static friction, which is in contradiction with the assumptions of Coulomb's static friction model. This inaccuracy must be attributed to numerical error, most likely due to the basic property of the penalty method, which always produces a certain amount of violation of the enforced constraints (i.e. penetration). However, the value of this error is obviously not very significant and the accuracy of the obtained result can be considered as satisfactory.

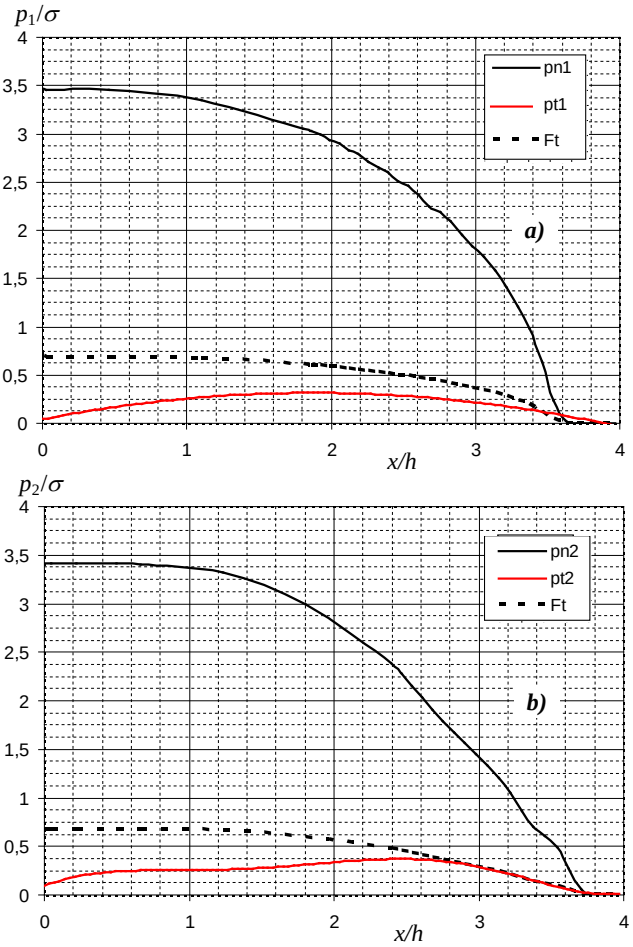

Fig. 7. *Contact pressure distributions for R/h = 500;*
a) at the indenter-layer interface a/h ≈ 3.97, $p_{n1,max}/\sigma \approx 3.46$;
b) at the layer-substrate interface b/h ≈ 3.98, $p_{n2,max}/\sigma \approx 3.42$

Based on the results presented in Figures 4-7 and comparing them to the results presented in Fig. 3 and Table 1, it can generally be concluded that the presence of friction reduces the maximal values of the normal component of the contact pressures and also contributes to the widening of the contact area. This phenomenon holds true on both contact surfaces. The one exception to this conclusion seems to be the case of indenter-layer interface when $R/h = 50$, since the result for the contact area is larger for the frictionless case. This result may well be the consequence of numerical error in either of the two cases and should be further scrutinized.

The tangential contact tractions p_t follow a consistent pattern for all geometries with regard to stick and slip zones. At the indenter-layer interface all points are in a state of stick, since the static friction force exceeds the value of the tangential contact tractions. At the layer-substrate interface points enter a state of slip in the area away from the centre, where the points remain in a state of stick. This result is in qualitative agreement with those in the available literature. Moreover, the extent of the stick zone relative to the size of the entire layer-substrate contact area increases as the ratio R/h increases. The size of the stick zone $(x/h)_{st}$ relative to the size of the contact area b is estimated in Table 2.

Table 2. *Relative size of the stick zone for all values of R/h*

R/h	50	100	200	500
$\frac{1}{b}\left(\frac{x}{h}\right)_{st}$	0.28	0.30	0.44	0.70

It is evident from Table 2 that the extent of the stick zone grows progressively as R/h increases.

It should, however, be noted that the values in Table 2 are approximate, since the curves obtained for tangential contact pressures contain a certain amount of error, as already pointed out.

4. Conclusion and outlook

The behaviour of receding contacts with a single unbonded layer was studied under the assumption of frictional contact. The influence of friction was analysed on a preliminary level, with emphasis on qualitative assessment, and four geometries with $R/h = 50$, 100, 200 and 500 were analysed with the coefficient of friction assumed to be 0.2 on both contacting surfaces. The problem was modelled within the framework of linear elasticity and all three bodies were considered as elastic. Such level of generality in the model presents a novelty in this field of study.

The obtained results show that the presence of friction reduces the values of the normal component of maximal contact pressures on both contact surfaces, at the same time widening the contact areas. Friction was modelled in accordance with Coulomb's static friction model, so the criterion for the determination of stick and slip zones was the equality of the local tangential contact traction and the local static friction force. At the indenter-layer interface all points remain in a state of stick, since the static friction force exceeds the value of the tangential contact tractions. However, at the layer-substrate interface points in the area away from the central point of contact, i.e. toward the edges of the contact area, enter a state of slip, while still remaining in a state of stick in the vicinity of the central point. In fact, the size of the stick zone $(x/h)_{st}$ relative to the size of the entire contact area is shown to grow progressively as R/h increases.

Potential extensions and improvements of the presented study are many. Firstly, the problem should be investigated for a larger set of values of the coefficient of friction. Secondly, it is a worthwhile effort to analyse the load-dependent aspects of the problem, which would quantify the variable nature of the stick and slip zones within the same geometry analysed for a single coefficient of friction. The investigation for several different coefficients of friction and several geometries would then fully characterize the receding contact of a single unbounded layer. Finally, possible numerical errors, which are always present, should be put under additional scrutiny in order to fully validate the presented results and observations.

References

[1] Johnson, K. L. *Contact mechanics*, Cambridge University Press, Cambridge, 1992.

[2] Filon, L. N. G. *On an Approximate Solution for the Bending of a Beam of Rectangular Cross-Section under any System of Load, with Special Reference to Points of Concentrated or Discontinuous Loading*. Philosophical Transactions of the Royal Society of London, 1903, A 201, pp. 63-155.

[3] Keer, L. M.; Dundurs, J.; Tsai, K. C. *Problems Involving a Receding Contact Between a Layer and a Half Space*. Transactions of the ASME – Journal of Applied Mechanics Vol. 39 (4), 1972, Series E, pp. 1115-1120.

[4] Tsai, K. C.; Dundurs, J.; Keer, L. M. *Elastic Layer Pressed Against a Half Space*. Transactions of the ASME – Journal of Applied Mechanics Vol. 41 (3), 1974, Series E, pp. 703-707.

[5] Gladwell, G. M. L. *On Some Unbonded Contact Problems in Plane Elasticity Theory*. Transactions of the ASME – Journal of Applied Mechanics Vol. 43 (3), 1976, Series E, pp. 263-267.

[6] Durelli, A. J.; Parks, V. J.; Nørgård, J. S. *Photoelastic solution of stresses in the elastic foundation supporting a plate*. International Journal of Solids and Structures Vol. 9, 1973, pp. 193-202.

[7] Ahn, Y. J.; Barber, J. R. *Response of frictional receding contact problems to cyclic loading*. International Journal of Mechanical Sciences Vol. 50, 2008, pp. 1519-1525.

[8] Comez, I. *Frictional contact problem for a rigid cylindrical stamp and an elastic layer resting on a half plane*. International Journal of Solids and Structures Vol. 47, 2010, pp. 1090-1097.

[9] Adibelli, H.; Comez, I.; Erdol, R. *Receding contact problem for a coated layer and a half-plane loaded by a rigid cylindrical stamp*. Archives of Mechanics Vol. 65 (3), 2013, pp. 219-236.

[10] Öner, E.; Yaylaci, M.; Birinci, A. *Solution of a receding contact problem using an analytical method and a finite element method*. Journal of Mechanics of Materials and Structures Vol. 9 (3), 2014, pp. 333-345.

[11] Birinci, A.; Adiyaman, G.; Yaylaci, M.; Öner, E. *Analysis of continuous and discontinuous cases of a contact problem using analytical method and FEM*. Latin American Journal of Solids and Structures Vol. 12 (9), 2015, pp. 1771-1789.

[12] Öner, E.; Yaylaci, M.; Birinci, A. *Analytical solution of a contact problem and comparison with the results from FEM*. Structural Engineering and Mechanics Vol. 54 (4), 2015, pp. 607-622.

[13] Rončević, B.; Bakić, A.; Kodvanj, J. *Numerical and experimental analysis of a frictionless receding contact between cylindrical indenter, layer and substrate*. Transactions of FAMENA, 40, 2(2016), pp. 1-18.

[14] Allahabadi, R. *Three Dimensional Slideline Contact*. MSC/ /NASTRAN World User's Conference, 1993.

[15] MSC.Nastran 2004 Quick Reference Guide. MSC.Software Corporation, 2003.